Polarization-strain coupling in the mixed ferroelectric $KTa_{1-x}Nb_xO_3$

L. A. Knauss,* X. M. Wang, and J. Toulouse
Physics Department of Lehigh University, Bethlehem, Pennsylvania 18015-3184
(Received 14 June 95)

The peculiar polar properties of $KTa_{1-x}Nb_xO_3$ (KTN) are determined by the presence of electric dipoles associated with randomly distributed Nb off-center ions. Because the latter also possess an elastic quadrupole, they should permit a coupling between electric polarization and strain. In order to investigate this coupling, we have carried out an ultrasonic study of KTN for different Nb concentrations. The elastic constants C_{11} and C_{44} and the corresponding attenuations have been measured in the presence of dc bias electric fields of varying strengths. These fields were also applied in different directions relative to the acoustic polarization of the ultrasonic waves. The present ultrasonic results confirm the formation of polar nanoregions at $T^* \cong T_c + 20$ K, marking the transition to a strong-coupling regime. They can be described by a microscopic model in which the primary polarization fluctuations are associated with the collective reorientations of the Nb off-center ions within a polar nanoregion. These fluctuations and their coupling to the sound waves can be enhanced or depressed by a dc bias electric field. An E^2 dependence of the elastic constant indicates the electrostrictive nature of the coupling.

I. INTRODUCTION

The mixed ferroelectric $KTa_{1-x}Nb_xO_3$ (KTN) is a very interesting example of highly polarizable systems in which a strong electrostriction is induced by off-center ions. KTN crystallizes with the perovskite structure, typical of many ferroelectrics in which the central atom (Ta or Nb) is covalently bonded to the face-centered oxygens. Its parent system $KTaO_3$, although possessing a soft mode and therefore being highly polarizable, does not become ferroelectric. Most likely for bonding reasons, because of its electronic structure, Nb in KTN has been shown to reside off center, even above T_c, in one of eight $\langle 111 \rangle$ directions,[1] thus possessing a dipole moment. Due to the high polarizability of the $KTaO_3$ host, each dipole polarizes the surrounding region, thus forming what we shall call a polar cluster. The reorientation of the polar cluster thus corresponds to polar fluctuations that have been observed in dielectric and polarization[2] and in Raman scattering measurements.[3] At high temperature, the dielectric constant has been shown to follow a Curie-Weiss (CW) law $\epsilon \sim C/(T-T_0)$, with $T_0 > T_c$. At $T^* \cong T_c + 20$ K, the dielectric constant deviates from the CW behavior and exhibits "reduced softening."[4] At approximately the same temperature, the appearance of a symmetry-forbidden nonpolar mode in the Raman spectra indicates the growth of quasistatic distortions.[5] The concurrent observation of odd harmonics in the electric polarization suggests the occurrence, at that temperature, of a condensation of the dynamic polar clusters into slow-relaxing polar nanoregions (40–60 Å).[4]

Besides a dipole moment, off-center Nb ions also necessarily possess an elastic quadrupole moment that is inseparably linked to their electric dipole moment. A reorientation of one necessarily reorients the other, hence providing the basis for a coupling between polarization and strain and a strong electrostrictive effect.

In a previous publication, we reported on the temperature dependence of the longitudinal elastic constant C_{11} of KTN.[6] For intermediate concentrations and at high temperatures, C_{11} exhibits a pronounced softening, revealing a strong electrostrictive coupling between polarization fluctuations and a longitudinal strain. In another publication,[7] C_{11} and C_{44} were shown to be strongly influenced by an external dc bias field applied perpendicular to the direction of propagation of the wave but only within 20 K of the transition. In the present paper we have extended these measurements of C_{11} and C_{44} to several niobium concentrations and to fields applied in different directions relative to both the direction of propagation ($\vec{k}$) and the polarization direction ($\vec{p}$) of the acoustic wave. We also propose a microscopic model to explain the coupling of this wave to the polarization fluctuations at higher temperature and to the strains induced by the formation of polar nanoregions, closer to the transition.

Finally, KTN at high concentrations has been shown to undergo three successive transitions, each marked by a peak in the dielectric constant. At low concentrations, however, only one peak is observed in the dielectric constant,[8] suggesting the occurrence of a single transition from the cubic to the rhombohedral phase.[9] Here we use the field dependence of the ultrasonic measurements to gain some insight into the number and character of the transition(s).

II. EXPERIMENTAL RESULTS

The experimental system made use of an ultrasonic pulse echo technique with superheterodyne phase detection and an intermediate frequency (IF) of 60 MHz. The setup has been previously described in detail.[10] For each temperature run, a single absolute transit time was made and relative changes in the transit time were recorded thereafter. The precision of the absolute and relative measurements was typically 0.5% and 0.005%, respectively.

0163-1829/95/52(18)/13261(8)/$06.00

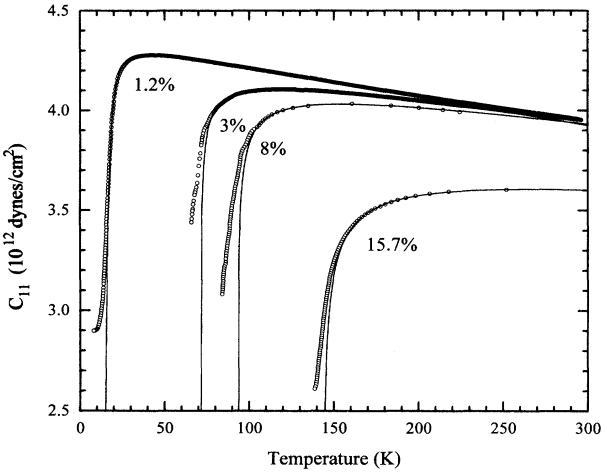

FIG. 1. Elastic constants C_{11} for four compositions of KTN. A fitting of the data to Eq. (1) is represented by solid lines.

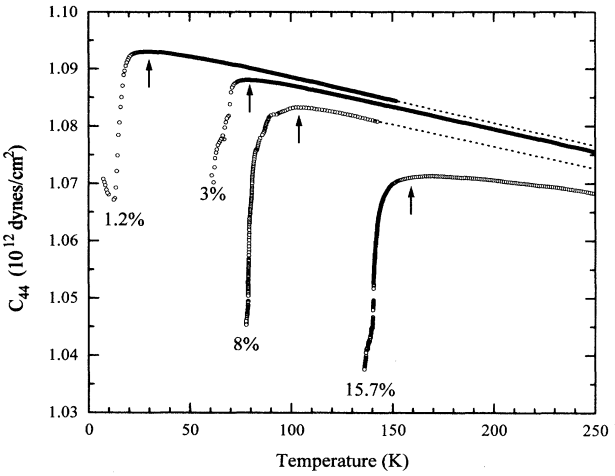

FIG. 2. Elastic constants C_{44} for four compositions of KTN. The arrows mark $T^* \cong T_c + 20$ K.

The measurements were performed on four different crystals with Nb concentrations of 15.7%, 8%, 3.5%, and 1.2% grown by a flux method. All crystals were approximately 1 cm^3 in size. They were cut with [100] or [110] faces polished flat and parallel to within 0.000 05″. Aluminum electrodes were deposited by evaporation, in order to apply the electric field, and 15-MHz $LiNbO_3$ transducers were bonded onto the appropriate faces with Nonaq stopcock grease. For the measurements, the crystals were placed in a cryostat with continuous He transfer. The temperature was monitored and controlled with two separate Si diode sensors and a Lake Shore temperature controller.

A. Zero-field measurements

The elastic constants C_{11} and C_{44} were measured in crystals with the four different concentrations listed above. The C_{11} and C_{44} results are presented in Figs. 1 and 2. A qualitative observation of these results reveals that the elastic constant C_{11} exhibits a softening far above the transition and the higher the concentration the farther in temperature this softening extends. By contrast, C_{44} exhibits softening in a much narrower temperature range above the transition. For the quantitative analysis of the results, the C_{11} curves in Fig. 1 have been fitted with the following expression:[11]

$$C_{11}=A_1+A_2T-A_3(T-T_0)^{-n}. \quad (1)$$

The first two terms describe the normal anharmonic behavior and the third term describes the critical softening due to critical fluctuations. The exponent n was earlier predicted to be 0.5 for three-dimensional (3D) fluctuations, 1 for 2D fluctuations, and 1.5 for 1D fluctuations.[12] The fitted curves are in good agreement with the experimental ones at high temperature, but depart from these when approaching the transition. During the fitting procedure, all the parameters in Eq. (1) were allowed to vary except for the 15.7% crystal for which T_0 was fixed in accordance with the dielectric results. The parameters obtained from the C_{11} fits are given in Table I. In view of their values, two main remarks can be made. First, an exponent of 0.5 was obtained for the three higher concentrations, corresponding to 3D fluctuations and in agreement with the Curie-Weiss behavior observed in the dielectric measurements. For the 1.2%, in which the softening is weaker at high temperature, a good fit was only obtained with an exponent close to 2. Second, the transition temperatures T_0 obtained from the fits are all greater than the observed transition temperatures. Therefore, upon approaching the transition, the elastic constant C_{11} softens less than what would be expected from an extrapolation of its high-temperature behavior which is dominated by dynamical fluctuations of the order parameter; i.e., the fluctuations do not diverge.

The C_{44} results are presented in Fig. 2. As seen with C_{11}, a significant softening of C_{44} is apparent. In contrast to C_{11}, however, this softening is not expected in perovskite

TABLE I. Parameters obtained from fitting C_{11} for several compositions of KTN. Fitted values of the parameters A_1, A_2, A_3, T_0, and p from Eq. (1).

	A_1 ($\times 10^{12}$)	A_2 ($\times 10^9$) (dyn/cm^2)	A_3 ($\times 10^{12}$)	T_0 K	p
1.2%	4.3568	1.4384	22.8383	11.77	2.1
3.0%	4.3632	1.2150	0.7972	70.93	0.5 [a]
8.0%	4.3395	1.1106	1.0746	92.63	0.5 [a]
15.7%	3.9339	0.6424	1.7527	143 [a]	0.5 [a]

[a]Fixed parameter.

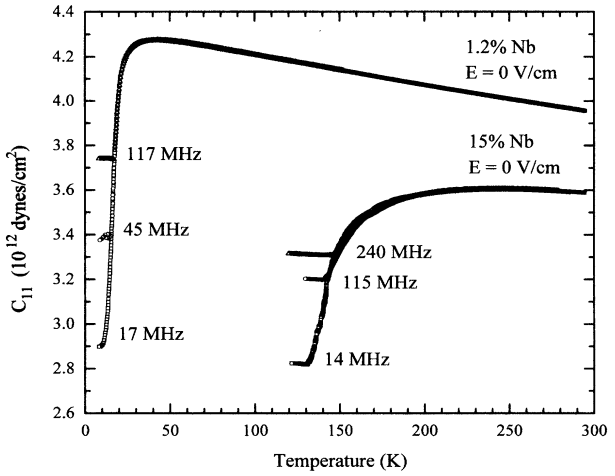

FIG. 3. Elastic constants C_{11} for several frequencies and two compositions of KTN.

ferroelectrics which usually first transform to a tetragonal phase. Here, in fact, C_{44} is only observed to soften close to the transition, and, interestingly, starting at $T^* \cong T_c + 20$ K where C_{11} deviates from its high temperature behavior in Fig. 1.

The frequency dependence of the elastic constant C_{11} has also been studied. The results are presented in Fig. 3 for two very different concentrations. No frequency dispersion whatsoever could be detected on this figure, although the measurements at higher frequencies do not extend to lower temperatures. This latter limitation is due to the fact that the attenuation α, which usually goes as ω^2, is greater and that the signal therefore falls below the level of detectability earlier for higher frequencies.

The attenuation for longitudinal waves corresponding to the elastic constant C_{11} is shown in Fig. 4 for different concentrations. This attenuation is seen to increase in a steplike fashion, starting precisely, again, at the "deviation temperature" previously identified on the C_{11} and the C_{44} curves.

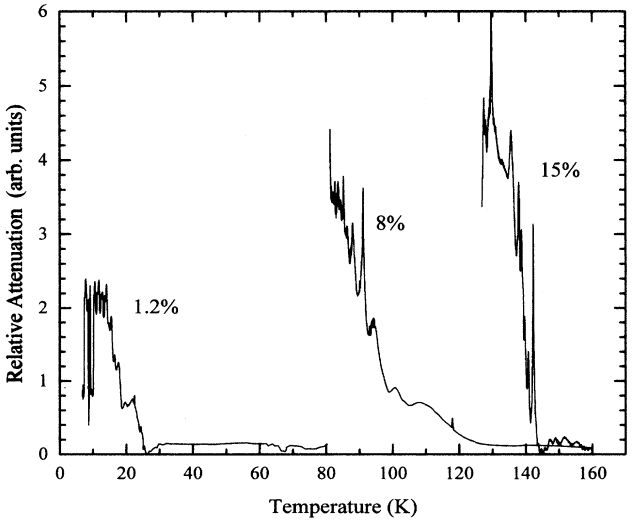

FIG. 4. Relative attenuation for three compositions of KTN.

All the above ultrasonic results are quite consistent with the dielectric, polarization, and Raman results obtained on crystals from the same boules and described in the Introduction. We briefly compare them here, keeping a more detailed comparison for the discussion section. At high temperature, the dielectric constant follows a Curie-Weiss law and the present ultrasonic results correspondingly indicate a mean-field type of coupling between strain and 3D dynamic polar fluctuations. The Curie-Weiss temperature found from the present ultrasonic measurements agrees well with that found from the dielectric measurements. At $T^* \cong T_c + 20$ K, both the dielectric and elastic constant C_{11} deviate from their above corresponding behaviors and exhibit "reduced softening." This reduced softening has recently been shown[4] to be due to the condensation of dynamic polar clusters into polar nanoregions. This corresponds quite well to the present ultrasonic results; the formation of these regions will necessarily be accompanied by local strains that can couple to sound waves resulting in a reduced softening of the elastic constant C_{11} and a rising attenuation. The concurrent softening of the elastic constant C_{44} is attributed to the fact that, because the local distortion is most likely tetragonal and because the distortion axis is randomly distributed amongst the three cubic directions, the lattice is likely to accommodate the strains via softening towards a rhombohedral distortion.

B. Field dependence

The zero-field ultrasonic measurements having revealed a coupling between strain and polarization, it appeared important to carry out measurements in the presence of a dc bias field. The purpose of the electric field was to modify this coupling and thereby obtain more quantitative information about it. dc fields were consequently applied parallel and perpendicular to the wave vector of longitudinal and transverse acoustic wave propagating along the [100] and [110] directions of the crystals. The crystals investigated in this part of the study were the 1.2% Nb crystal with [100] external faces and two high concentration crystals, a 15.7% Nb crystal with [100] external faces and a 15% Nb crystal with four [110] and two [001] external faces.

The effect of a dc field can be understood on the basis of a microscopic model. In order to facilitate the interpretation of the experimental results, we describe the model for each separate configuration of the acoustic wave vector polarization and dc bias electric field. However, in order to justify the applicability of this microscopic model to ultrasonic results, it is important to note the following remark.

The wavelength of sound being much longer than the average size of the nanoregions, the ultrasonic strain can be regarded as uniform across a given nanoregion. Within a given nanoregion, the motion of Nb ions and that of surrounding Ta ions are strongly correlated and, under a uniform strain, these ions will all move in unison. The model can therefore be described at the level of a single unit cell in which the polarization fluctuations are associated with the local reorientation of a single niobium ion.

1. C_{11} under dc bias fields

Relatively low fields are required on low Nb concentration crystals. On the 1.2% Nb crystal, fields of 0, 150, and

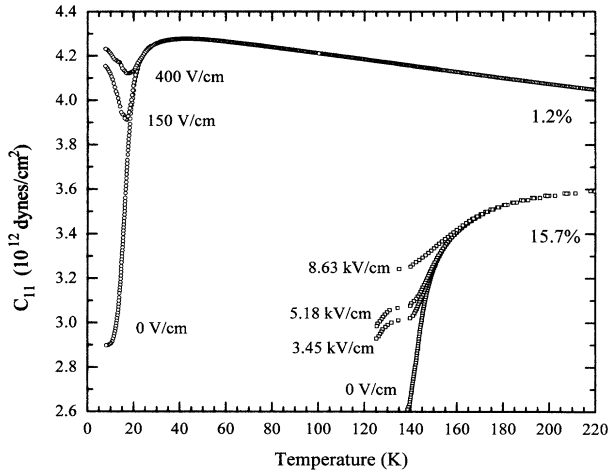

FIG. 5. Elastic constants C_{11} for 1.2% and 15.7% KTN in the presence of several dc bias electric fields. The electric fields were applied parallel to the propagation direction of the acoustic waves.

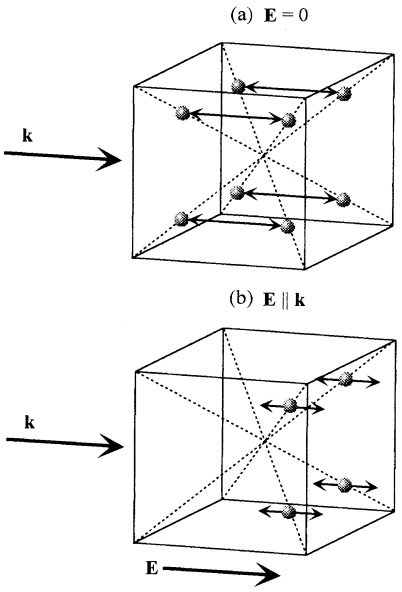

FIG. 6. Model for the coupling of longitudinal acoustic waves to polar fluctuations for (a) the zero-field case and (b) with a dc bias electric field **E** applied parallel to the propagation direction of the acoustic wave, **k**.

400 V/cm were applied parallel to the wave vector of the longitudinal acoustic wave propagating in the [100] direction of the crystal. For the 15% and 15.7% Nb crystals, the configuration was identical but the fields were 20 times larger, successively 0 V/cm and 3.45, 5.18, and 8.63 kV/cm.

The results are presented in Fig. 5 and show that C_{11} hardens significantly under the influence of the field. Also under the influence of the field, the single apparent transition in the 1.2% Nb crystal is shifted towards higher temperatures. This is also the case in the 15.7% Nb although it is not as conspicuous. Finally, we note that the effect of the field is felt primarily in the lower-temperature region where polar nanoregions are already present.

As shown in Fig. 6(a) for the zero-field case, a longitudinal sound wave can couple to polar fluctuations (indicated by arrows) in the direction of propagation. However, when the field is applied in the same direction [Fig. 6(b)], the fluctuations are suppressed, effectively hardening the lattice or decreasing the elastic susceptibility, i.e., increasing the elastic constant.

The field dependence of C_{11} is presented in a more meaningful form in Fig. 7(a) for the 15.7% Nb crystal, as a function of E^2. Despite the limited number of points C_{11} appears to vary quadratically with the field, $C_{11} \sim B(T)E^2$, for fields greater than approximately 3 kV/cm. The same behavior has been observed for the 1.2% Nb crystal. The coefficient $B(T)$ is shown for both concentrations in Fig. 7(b), which clearly demonstrates that the onset of the field effects does indeed coincide with the appearance of the polar nanoregions at $T^* \cong T_c = 20$ K.

2. C_{44} under dc bias fields

The elastic constant C_{44} in the presence of a dc bias field was measured on two crystals. The first one was again the 1.2% used above but the second was the 15% Nb crystal mentioned earlier with four [110] and two [001] external faces. The reason for the switch to this latter crystal was that the 15.7% Nb crystal spontaneously cleaved at the end of the final C_{11} measurement, under a dc field of 8.6 kV/cm. We then had to use 15% Nb crystal. Because of the different external faces of the 1.2% Nb and the 15% Nb crystals, we present each set of results in turn.

a. KTN 1.2% Nb. For the C_{44} measurements on the 1.2% Nb crystal, the field was also applied parallel to the wave vector of the transverse acoustic wave propagating in the [100] direction and polarized in the [001] direction. The results are presented in Fig. 8.

Opposite to the behavior of C_{11}, the softening of C_{44} is enhanced by the field. Also, under the influence of the field, the single apparent transition is shifted towards lower temperatures, showing again opposite behavior to that of C_{11}. For the same reasons as those given previously, we can use a microscopic model to explain the C_{44} results. As illustrated in Fig. 9(a), in the zero-field case and under the shear strain of the transverse acoustic wave, the minimum energy positions for the Nb ion are located on two of the four cube diagonals. The only possible polar fluctuations that could couple to the acoustic wave would then involve jumps between next-nearest-neighbor positions and these jumps can be expected to have a low probability. Thus the transverse acoustic wave itself suppresses the fluctuations and effectively stiffens the lattice. However, when the field is applied in the direction of propagation, as shown in Fig. 9(b), the potential energy of niobium in the two upper positions on the right becomes again comparable to that in the two lower positions and the transverse wave can again couple to polar fluctuations. Thus, in the presence of the field, the lattice softening exhibited by the elastic constant C_{44} is enhanced.

b. KTN 15% Nb. For the C_{44} measurements on the 15% crystal, the transverse acoustic wave was propagated along the [100] direction and polarized along the [001] direction. In the first experiment the field was applied along [001] ($\perp \mathbf{k}$) and in the second experiment along [110], i.e., in the direction of propagation ($\| \mathbf{k}$), as shown in Fig. 10. The re-

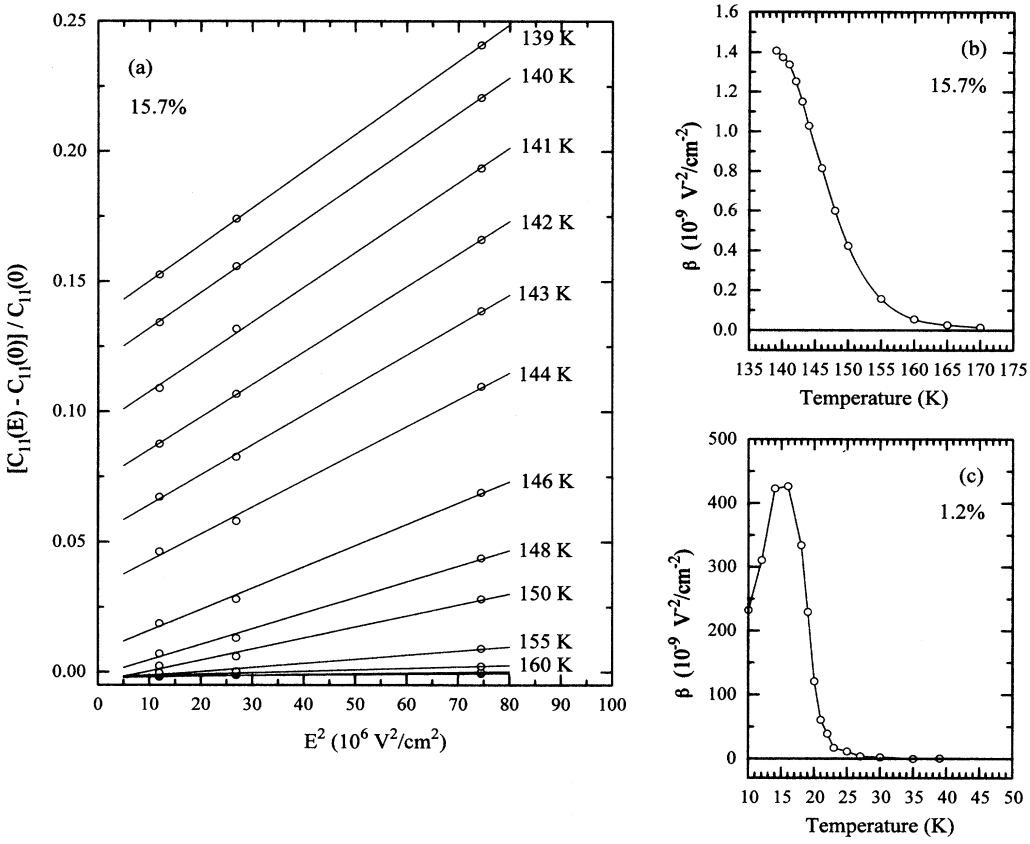

FIG. 7. (a) Quadratic field dependence of C_{11} for a concentration of 15.7% and temperatures ranging from 139 to 170 K. The coefficient of proportionality, β, is presented as a function of temperature for (b) the 15.7% and (c) the 1.2% concentrations.

sults of the two experiments are strikingly different. Upon applying the field in the [001] direction, the fluctuations are suppressed while upon applying it in the [110] direction a remarkable result is obtained. Not only are fluctuations enhanced such that the softening of C_{44} is multiplied by a factor of 20, but all signs of intermediate transitions disappear as the system continuously goes from the cubic to the rhombohedral phase. (See inset.) These results can again be explained with the microscopic model used previously and illustrated in Fig. 11 for the present configuration. When the field is applied along [001][Fig. 11(b)], as in the first experiment, the Nb ions will occupy one of the four lower positions thus made energetically favorable. (For simplicity, only two positions are indicated in the figure.) Consequently polar fluctuation along the vertical axis will be suppressed. However, when the field is applied along [110] [Fig. 11(c)], the Nb ions will preferentially occupy the two positions connected by arrows which can be coupled by the transverse acoustic wave polarized along [001]. In this configuration the polar fluctuations are most enhanced because the only allowed Nb jump or fluctuation is the one that couples to the transverse acoustic wave. Moreover, this fluctuation is also the one leading to the rhombohedral distortion, thus explaining why, in this configuration, the higher transitions are no longer resolved and the crystal goes continuously from the cubic to the rhombohedral phase.

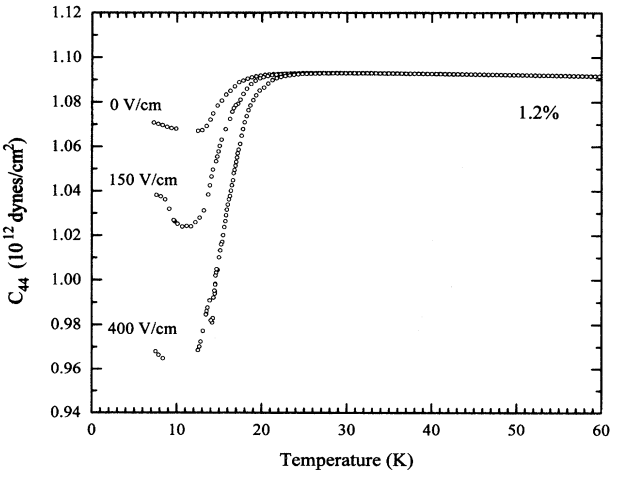

FIG. 8. Elastic constants C_{44} for 1.2% KTN in the presence of two dc bias electric fields. The electric fields were applied parallel to the propagation direction of the acoustic waves.

In all the lattice diagrams used above, a single unit cell has been represented for ease of illustration. It should be clear, however, that this unit cell stands for all the unit cells

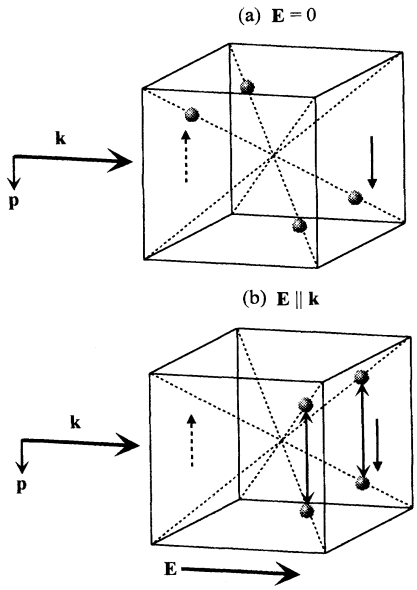

FIG. 9. Model for the coupling of transverse acoustic waves, propagating in a [100] direction, to polar fluctuations for (a) the zero-field case and (b) with a dc bias electric field **E** applied parallel to the propagation direction of the acoustic wave, **k**. The polarization axis of the acoustic wave is represented by **p**.

of a nanoregion in which, as we have mentioned earlier, the strain will be approximately uniform.

III. DISCUSSION

A. Zero-field ultrasonic results

Based on the above ultrasonic results, one can distinguish two dynamics regimes. At high temperature, the elastic constant C_{11} softens as $(T-T_0)^{-0.5}$, in accordance with a mean-field model in which the longitudinal acoustic wave couples to 3D dynamic fluctuations of the order parameter, here the polarization; the lattice dynamics display a purely displacive character. We note, however, that $T_0 > T_c$. The same behavior has been observed in a dielectric study of crystals with the same nominal concentrations in which the dielectric constant was found to follow a Curie-Weiss law also with $T_0 > T_c$.[4] In this region, C_{44} does not show any softening and neither longitudinal nor transverse waves show any attenuation.

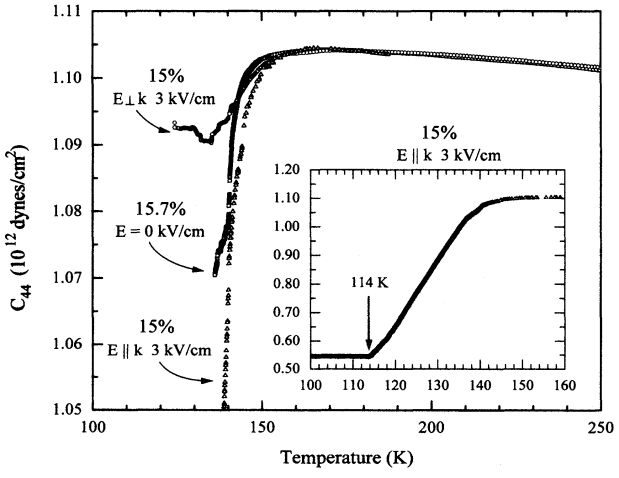

FIG. 10. Elastic constants C_{44} for 15% and 15.7% KTN in the presence of one dc bias electric field and zero electric field. The electric field was applied both parallel and perpendicular to the propagation direction [110] of the acoustic waves. The inset shows all the data for the field parallel case which continues to decrease with temperature down to 114 K.

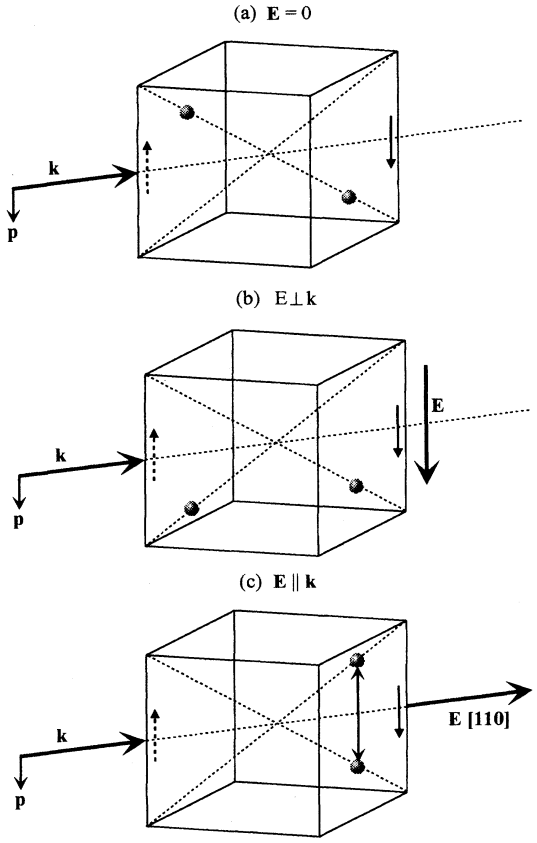

FIG. 11. Model for the coupling of transverse acoustic waves, propagating in a [110] direction, to polar fluctuations for (a) the zero-field case, (b) with a dc bias electric field **E** applied perpendicular to the propagation direction of the acoustic wave, **k**, and (c) with a dc bias electric field **E** applied parallel to the propagation direction. The polarization axis of the acoustic wave is represented by **p**.

At approximately $T_c + 20$ K for any concentrations, C_{11} deviates from the above mean-field behavior, C_{44} rapidly softens, and the attenuation increases in a steplike manner. The reduced softening of C_{11} and the increasing attenuation clearly reveal the appearance of strains in the crystal, which coincides with a rise in the remanent polarization and in the coercive field measured from hysteresis loops. This is shown in Fig. 12 for the 15.7% crystal but is also true for other concentrations, including 1.2% Nb. The present observation of an increasing strain strengthens significantly our recent interpretation of dielectric and polarization results in terms of a cooperative condensation.[4]

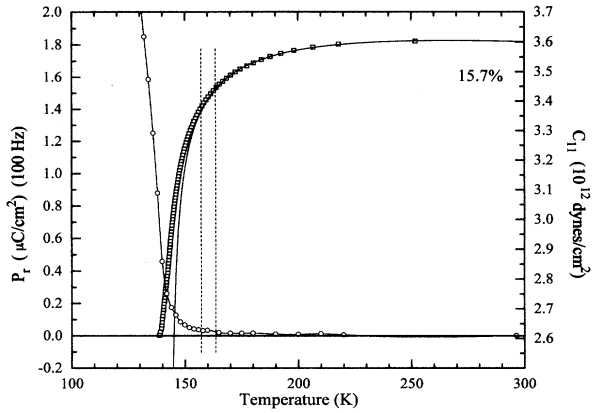

FIG. 12. The remanent polarization, measured at 100 Hz, and the elastic constant C_{11}, measured at zero electric field, for a composition of 15.7% KTN plotted as a function of temperature. The fitting results of C_{11} are indicated by the solid curve. The dotted lines represent the temperature range over which the C_{11} fitting deviates from the measured values and the remanent polarization starts to increase rapidly.

At $T^* \cong T_c + 20$ K the real part of the dielectric constant was found to deviate from a Curie-Weiss law while the imaginary part exhibited a peak with only very little frequency dependence in position. Also, most significantly, odd harmonics were found to appear in the ac polarization. A detailed analysis of the TO_2 Raman line near T_c also indicated the presence of polar nanoregions approximately 60 Å in size.[5] The present ultrasonic data therefore confirm the condensation of dynamic clusters into quasistatic nanoregions; it is the formation of these nanoregions that results in the reduced softening of the elastic constant C_{11} and in the increased attenuation observed. As we mentioned earlier, the softening of the elastic constant C_{44}, also triggered by this formation, is attributed to the existence of three variances of the tetragonal distortion which can be simultaneously accommodated by a softening of the lattice towards a rhombohedral distortion.

Further polarization measurements have also revealed low-frequency relaxation processes[13] (from several Hz to kHz), indicating that these nanoregions, although stable, can nevertheless reorient, albeit slowly. The absence of a frequency dispersion at all temperatures in the present ultrasonic measurements suggests that either this reorientation is a 180° process, such that the elastic distortion remains unchanged by it, or else it takes place a frequencies lower than MHz. Recent dielectric measurements over a broad frequency range seem to support this latter explanation.[14]

B. Field dependence

1. Electrostriction

As illustrated in Figs. 5, 8, and 10, the field begins to have an effect on the elastic constants primarily at T^*, namely, upon the formation of the polar nanoregions. This is even clearer in Fig. 7 where the field dependence of $\Delta C/C$ was presented as a function of E^2:

$$\Delta C_{11}/C_{11} \equiv \frac{C_{11}(E) - C_{11}(0)}{C_{11}(0)} = B(T)E^2.$$

In the inset, the temperature dependence coefficient $B(T)$, which is an electrostrictive coefficient, begins to increase at 165 K for the 15.7% Nb crystal and at 30 K for the 1.2% Nb crystal, albeit approximately 20 K above the transition for both. Based on these observations, we conclude that the formation of polar nanoregions in KTN gives rise to strong electrostrictive effects.

2. Transition(s) in low concentration KTN

Another aspect of the field dependence has to do with the transition temperature(s). This is particularly interesting in low concentration KTN in which the observation of a single peak in the dielectric constant had led earlier to the conclusion of a single transition from the cubic directly to a rhombohedral phase.[8] At high concentrations ($x \gtrsim 5\%$), KTN undergoes three successive transitions, cubic tetragonal, tetragonal orthorhombic, and orthorhombic rhombohedral, each of them marked by a separate peak in the dielectric constant.

It was pointed out in Figs. 5 and 8 for KTN 1.2% Nb that the application of a field $\mathbf{E}\|\mathbf{k}$ shifts the C_{11} minimum towards higher temperatures but the C_{44} minimum towards slightly lower temperatures relative to their zero-field position. The specific character of each of the two elastic constants C_{11} and C_{44} can explain the above observations concerning their respective minima and the transition temperatures that they indicate. The elastic constant C_{11} is a measure of the susceptibility of the crystal to a tetragonal strain. As can be seen in Fig. 6, the application of a dc bias electric field $\mathbf{E}\|(100)$ depresses the fluctuations and stabilizes the tetragonal distortion, hence leading to a shift of the C_{11} minimum towards higher temperatures. The stabilization of a larger tetragonal strain due to the presence of the field will also result in a shift of the rhombohedral transition towards lower temperatures. This is shown by the displacement of the C_{44} minimum towards lower temperatures. The shift of the C_{11} and C_{44} minima in opposite directions, under the influence of the field, suggests that initially, in zero field, the three transitions may be superposed. In fact, it is interesting to note that, for zero field, the C_{11} and C_{44} minima are rather flat and the curves resemble steps. As noted earlier there is some experimental uncertainty in the case of C_{11} because of the higher attenuation. As the field is increased, the minima become more pronounced, shifting in opposite directions, respectively for C_{11} and C_{44}. The flat minimum for zero field could indeed indicate a complex transition that is a combination or superposition of the several distinct transitions that are observed for higher concentrations.[14]

IV. CONCLUSION

Experimental evidence reported here regarding the large effect of a dc bias electric field on the elastic constants is an indication of the strong electrostrictive coupling that exists between polarization and strain in KTN. Using a microscopic model, we have been able to explain the specific effects of dc bias fields applied in different directions relative to the wave vector and polarization directions of longitudinal and trans-

verse acoustic waves. This model shows that the electrostrictive coupling is induced by the collective motion of off-center Nb within polar nanoregions, the existence of which had been demonstrated earlier.

The experimental evidence for the development of strains at $T^* \cong T_c + 20$ K is also important in that it strengthens the conclusions of a recent dielectric and polarization study.[4] In this study, we interpreted the results as indicating the occurrence of a condensation of dynamic polar clusters into polar nanoregions at T^*.

Finally, the present ultrasonic results suggest that, at low Nb concentrations, several transitions simultaneously take place, which can be separated by the application of a bc bias field.

ACKNOWLEDGMENTS

This work was partially supported by the Division of Materials Sciences, U.S. Department of Energy, under Contract No. DE-FG02-86ER 45258.

*Current address: Naval Research Laboratory, 4555 Overlook Ave. SW, Washington, DC 20375-5345

[1] O. Hanske-Petitpierre, Y. Yacoby, J. Mustre de Leon, E. A. Stern, and J. J. Rehr, Phys. Rev. B **44**, 6700 (1991).

[2] J. Toulouse, X. M. Wang, L. A. Knauss, and L. A. Boatner, Phys. Rev. B **43**, 8297 (1991); L. A. Knauss, Ph.D. thesis, Lehigh University, 1994.

[3] J. Toulouse, P. DiAntonio, B. E. Vugmeister, X. M. Wang, and L. A. Knauss, Phys. Rev. Lett. **68**, 232 (1992).

[4] J. Toulouse and R. Pattnaik, J. Phys. Chem. Solids (to be published).

[5] P. DiAntonio, B. E. Vugmeister, J. Toulouse, and L. A. Boatner, Phys. Rev. B **47**, 5629 (1993).

[6] X. M. Wang, J. Toulouse, and L. A. Boatner, Ferroelectrics **112**, 255 (1990).

[7] J. Toulouse, X. M. Wang, and L. A. Boatner, Solid State Commun. **68**, 353 (1988).

[8] D. Rytz and H. J. Scheel, J. Cryst. Growth **59**, 468 (1982).

[9] P. DiAntonio, X. M. Wang, J. Toulouse, and L. A. Boatner, Ferroelectrics **120**, 107 (1991).

[10] J. Toulouse and C. Launay, Rev. Sci. Instrum. **59**, 492 (1988).

[11] R. O. Bell and G. Rupprecht, Phys. Rev. **129**, 90 (1963); D. Rytz, A. Chatelain, and U. T. Hochli, Phys. Rev. B **27**, 6830 (1983).

[12] J. M. Courdille, J. Dumas, S. Ziolkiewicz, and J. Joffrin, J. Phys. (Paris) **12**, 1519 (1977).

[13] L. A. Knauss, B. E. Vugmeister, and J. Toulouse, Ferroelectrics **157**, 251 (1994).

[14] R. Pattnaik and J. Toulouse (unpublished).